Available online at www.sciencedirect.com
ScienceDirect
Ceramics International 37 (2011) 2095–2100
CERAMICS INTERNATIONAL
www.elsevier.com/locate/ceramint

Solid oxide fuel cells with YSZ-BNO Bi-layer electrolyte film deposited by magnetron sputtering

Sea-Fue Wang [a,*], Yung-Fu Hsu [a], Yu-Chia Huang [a], Wen-Cheng Wei [b]

[a] Department of Materials and Mineral Resources Engineering, National Taipei University of Technology, Taipei 10608, Taiwan, R.O.C
[b] Department of Materials Science and Engineering, National Taiwan University

Received 1 February 2011; received in revised form 16 February 2011; accepted 26 February 2011
Available online 8 April 2011

Abstract

Bi-layer electrolyte films of $Zr_{0.84}Y_{0.16}O_{1.92}$ (YSZ)- $0.79Bi_2O_3$-$0.21Nb_2O_5$ (BNO) were deposited by RF magnetron sputtering on NiO-SDC anode substrates. The stoichiometry of the BNO electrolyte film was found strongly dependent on the ratio of Ar and O_2 during sputtering, and the BNO film deposited at a mixture of 31 sccm Ar and 7 sccm O_2 appeared to be the closest to the target composition. When deposited at 300 °C and subsequently annealed at 700 °C, the BNO electrolyte emerged to be crack free and dense with some scattering closed pores. The XRD patterns of the film are indexed to the cubic Fm $\bar{3}$ m structure of Bi_3NbO_7. The as-deposited film was well-crystalline and consisted of fine grains and random orientation microstructures. For electrolyte thicknesses of approximately 4.0 μm YSZ and 1.5 μm BNO layers, the open circuit voltage (OCV) and the maximum power density of the single cell with Ag cathode read respectively 0.94 V and 10 mW/cm^2 at 600 °C. These OCV values are lower than the expected theoretical value due to the high partial electronic conductivity.

Keywords: Solid oxide fuel cell; Bi-layer electrolyte; Sputtering; Electrolyte

1. Introduction

Solid oxide fuel cells (SOFCs) are considered to have potential for commercialization thanks to their high energy conversion efficiency, self-reforming ability, compatibility with common hydrocarbon fuels, use of solid state materials, and no need of noble metals as catalysts [1]. SOFCs can be used in large-size stationary power facilities or applied to heat and power generation for home and factory as well as auxiliary power units for electrical systems in transportation vehicles. In recent years, enormous research efforts have been invested on the development of intermediate temperature SOFCs (IT-SOFCs) capable of operating at temperatures between 500 and 700 °C [2,3]. However, the performance of IT-SOFCs depends strongly on the ionic conductivity of the electrolyte and the polarization resistance (Rp) of the electrodes [4]. The former problem can be solved by using alternative electrolytes with higher ionic conductivity at low temperatures, such as $La_{0.9}Sr_{0.1}Ga_{0.8}Mg_{0.2}O_{3-\delta}$ (LSGM) and $Sm_{0.2}Ce_{0.8}O_{2-\delta}$ (SDC) or by using a thin yttria-stabilized zirconia (YSZ) electrolyte film [5].

Several film-deposition approaches have been used to reduce the thickness of electrolyte layers. These approaches can be divided into the following three categories: (a). Physical methods including sputtering [6], pulsed laser deposition (PLD) [7]; (b). Chemical processes including sol-gel [8], spray pyrolysis [9], atomic layer deposition (ALD) [10], electrochemical vapor deposition (EVD) [11], metalorganic chemical vapor deposition (MOCVD) [12], flame assisted vapor deposition [13], electrostatic assisted vapor deposition [14]; and (c). Ceramic powder processes including screen printing [15], tape casting [16], suspension spray coating [17], slurry spin-coating [18], inject printing [19], electrophoretic deposition [20], and dry pressing [21]. However, these processes are often marked with restrictions rendering large-scale SOFC manufacturing highly challenging, such as a high substrate temperature (typically around 700∼900 °C), sophisticated deposition and doping parameters, expensive precursors and

* Corresponding author. Present Address: Department of Materials and Mineral Resources Engineering National Taipei University of Technology, 1, Sec. 3, Chung-Hsiao E. Rd., Taipei, Taiwan 106, R.O.C.
Tel.: +886 2 2771 2171x2735; fax: +886 2 2731 7185.
E-mail address: sfwang@ntut.edu.tw (S.-F. Wang).

0272-8842/$36.00
doi:10.1016/j.ceramint.2011.02.022

processes, thickness inhomogeneity, low densification, large induced strain, or the need of multiple coatings and complex sintering procedures, difficulty of stoichiometry control, and high equipment cost. Among the film deposition methods, magnetron sputtering has been widely applied to deposit a variety of coatings aimed at improving electrical properties, optical properties, wear resistance, corrosion resistance, friction resistance, and appearance [22], many of which are of industrial importance.

In this study, the feasibility of deposition of $Zr_{0.84}Y_{0.16}O_{1.92}$ (YSZ)- $0.79Bi_2O_3$-$0.21Nb_2O_5$ (BNO) bi-layer electrolyte films on NiO-SDC anode substrates by RF magnetron sputtering method was investigated. The crystal structure and micro-structural evolution of the films were examined by X-ray diffraction (XRD) analysis and scanning electron microscopy (SEM). SOFC single cells were then built by screen printing an Ag cathode on the anode-supported substrates with YSZ-BNO bi-layer electrolyte. Microstructural and electrochemical performance studies of the SOFCs were then performed and discussed.

2. Experimental Procedure

Commercially available raw materials, including $Sm_{0.2}Ce_{0.8}O_{2-\delta}$ (SDC; Fuel Cell Materials, USA; $d_{50} = 0.53$ μm and BET surface area = 6.2 m^2g^{-1}), $Zr_{0.84}Y_{0.16}O_{1.92}$ (8YSZ; Fuel Cell Materials, USA; $d_{50} = 0.24$ μm and BET surface area = 6.31 m^2g^{-1}), and NiO (anode functional layer: Fuel Cell Materials, USA, $d_{50} = 0.8$ μm and BET surface area = 3.4 m^2g^{-1}; current collector layer: SHOWA, Japan, $d_{50} = 10.1$ μm and BET surface area = 0.06 m^2g^{-1}), were used. The anode-supported substrates incorporated a SDC electrolyte layer and a three-layer anode composed of a current collector layer (outer layer) of pure NiO and two functional layers of NiO-SDC composites with ratios of 60 wt%/40 wt% and 50 wt%/50 wt% respectively. The thin 50 wt% NiO/50 wt% SDC composite layer provided a good contact with the adjacent electrolyte layer. The preparation of the anode-supported substrates was described in a previous paper [23].

To prepared YSZ and BNO targets, $Zr_{0.84}Y_{0.16}O_{1.92}$ and $0.79Bi_2O_3$-$0.21Nb_2O_5$ powders were mixed in the methyl alcohol using polyethylene jars and ZrO_2 media. After drying, the powders were added with 3.5 wt% of a 15% PVA solution and then pelletized into disc shape at a uniaxial pressure of 2 tons/cm^2. The YSZ and BNO targets were then heat treated at 550 °C for 6 h to eliminate the PVA, followed by sintering at 1400 °C and 900 °C for 2 h, respectively. X-ray diffraction (XRD, Siemens D5000), scanning electron microscopy (SEM, JOEL JSM-T330A), and energy dispersive spectroscopy (EDS) on the sintered target surfaces were used to confirm the formation of phases and characterize the microstructures.

YSZ and BNO thin films were deposited on the anode substrates in sequence by RF magnetron sputtering using YSZ and BNO targets. Deposition of thin films was done in a sputtering system equipped with a turbomolecular pump to achieve a base pressure of $<2 \times 10^{-7}$ torr. For sputtering, argon as the working gas was at least 99.995% pure. Prior to deposition, the target was sputter–cleaned. Working pressure was in the range of $1x10^{-2}$ torr while RF power was 100 W. YSZ films were first deposited on the anode-supported substrates in an atmosphere of Ar and O_2 mixture with ratio of 30:1 and a bias of 45 V. During deposition, the substrate temperature was controlled at 300 °C. BNO films were subsequently deposited on the top of the YSZ films in an atmosphere of Ar and O_2 mixture with various ratios and with the substrate temperature ranging from room temperature to 300 °C. Film samples were heat treated at 650 °C in O_2 atmosphere in a RTA furnace (MILA-3000) at a heating rate of 1 °C/sec. XRD analysis was then performed, using a thin film diffractometer with monochromatic Cu Kα radiation, to examine the crystallographic evolution of films and to identify crystallized phase.

The anode-supported substrates with a YSZ-SDC bi-layer electrolyte deposited by sputtering were then screen printed to form an Ag cathode. Ag powders were mixed with a proper amount of terpineol (solvent) and ethyl cellulose (binder) to form a paste. The cathode was then fired at 650 °C for 2 h. Figure 1 shows the schematic drawing of the anode-supported single cell structure of SOFC with a YSZ-BNO bi-layer electrolyte layer deposited by RF magnetron sputtering, and Table 1 lists the dimensions of the single cell prepared in this study. The electrochemical performance of the single cell was measured at the set-up of a commercially available ProboStat (NorECs, Norway). The procedures of the electrochemical test were also described in a previous paper [23].

3. Results and Discussion

Deposition conditions of YSZ electrolyte film on the anode substrate via sputtering have been well investigated and reported in the literature [17,22], and the processing conditions

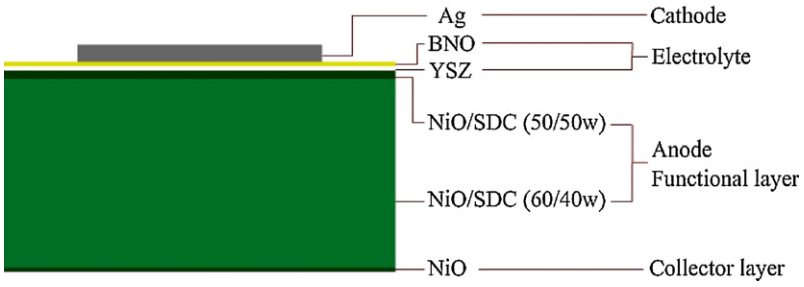

Figure 1. Schematic drawing of the anode-supported single cell structure of SOFC with a YSZ-BNO bi-layer electrolyte.

Table 1
Design of the anode supported single SOFC cell with YSZ-BNO bi-layer electrolyte.

Structure	Material	SOFC Cell
Cathode current collector layer	LSCF	40 μm
Electrolyte layer	YSZ	4.0 μm
	BNO	1.5 μm
Anode functional layer	NiO/SDC (50 wt%/50 wt%)	6 μm
Anode functional layer	NiO/SDC (60 wt%/40 wt%)	636 μm
Anode current collector layer	NiO	20 μm

from the literature were adopted as the sputtering parameters of YSZ films in this study. For optimizing the deposition of BNO on the NiO-SDC substrate, detailed investigation of the sputtering conditions, including atmosphere, substrate temperature, working pressure, and subsequent annealing, was performed. Table 2 shows the EMPA results of Bi and Nb ratios in the deposited films prepared at various flow rates of Ar and O_2. The stoichiometry of the BNO electrolyte film appeared to be strongly dependent on the ratio of Ar and O_2 during sputtering. The Bi and Nb ratio of the BNO film deposited at a mixture of 31 sccm Ar and 7 sccm O_2 read 78.89 m% and 21.11 m%, the closest to the target composition. Figure 2 shows parts of the XRD patterns of the BNO films deposited at various atmospheres compared with that of the BNO target. It indicated that only Bi_3NbO_7 phase existed in the target (Figure 2a). The diffraction peaks of the XRD patterns of the as-deposited films are indexed to the cubic Fm $\bar{3}$ m structure of Bi_3NbO_7 (JCPDS Card No. 86-0875, a = 0.5479 nm), which appears to be pretty similar to that of the target. It is consistent with that shown in the phase diagram [24]. 20 to 23 m% of Nb_2O_5 in the Bi_2O_3-Nb_2O_5, leads to the formation of Bi_3NbO_7 phase, a fcc phase similar to the high-temperature fcc δ-Bi_2O_3 phase. Bi_3NbO_7 is believed to exhibit a Type-II structure, which is an incommensurate modulation of the δ-Bi_2O_3 fluorite structure [25]. For the BNO films deposited at various atmospheres (Figure 2b), the XRD patterns seem very similar, though the Bi and Nb contents of the BNO films vary with the sputtering atmosphere.

Table 2
EMPA results of Bi and Nb contents in the deposited films prepared at various sputtering conditions.

Flow rate (sccm)		Working pressure (torr)	Power (W)	Bi: Nb ratio in the film
Ar	O_2			
32	4	1×10^{-2}	100	83.00: 17.00
32	6	1×10^{-2}	100	81.30: 18.70
32	7	1×10^{-2}	100	78.66: 21.34
32	8	1×10^{-2}	100	78.56: 21.44
32	10	1×10^{-2}	100	75.59: 24.41
31	7	1×10^{-2}	100	78.89: 21.11
30	7	1×10^{-2}	100	79.79: 20.21

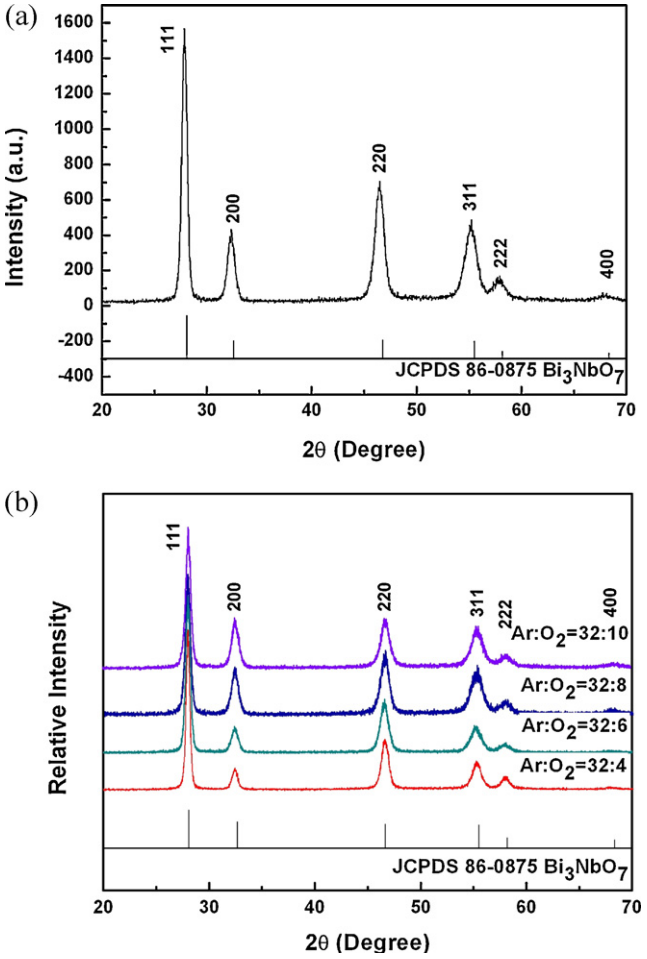

Figure 2. XRD patterns of (a) BNO target and (b) as deposited BNO films deposited using RF magnetron sputtering at various ratios of Ar and O_2.

Figure 3 shows the surface SEM micrographs of the BNO films deposited at the substrate temperatures of 25 °C and 300 °C in the as-deposited form as well as the micrographs of the films annealed at 700 °C for 2 h, and Figure 4 indicates the corresponding cross-section SEM micrographs. The annealing temperature of 700 °C was selected to examine the film deposition conditions and the film quality because the final cells with silver cathode was post-fired at 650 °C and operated at the temperature range of 500 to 700 °C. As shown in Figures 3(a) and 4(a), a uniform and dense BNO film approximately 7 μm in thickness was obtained under the sputtering conditions of O_2 flow rate of 7 sccm and Ar flow rate of 31 sccm on the unheated substrate. After annealing at 700 °C, mud cracks were observed on the surface of the film [Figure 3(b)], and the cracks occurred across the whole BNO layer until reaching the BNO-anode interface [Figure 4(b)]. Apparently, the cracks were induced by the difference in the thermal expansions of the BNO film and the anode substrate. The BNO film deposited at 300 °C is characterized by a greater surface roughness and a higher porosity, as indicated in Figure 3(c). After subsequent annealing at 700 °C, it could be observed that the BNO electrolyte was crack free and dense with some scattering closed pores [Figure 4(d)].

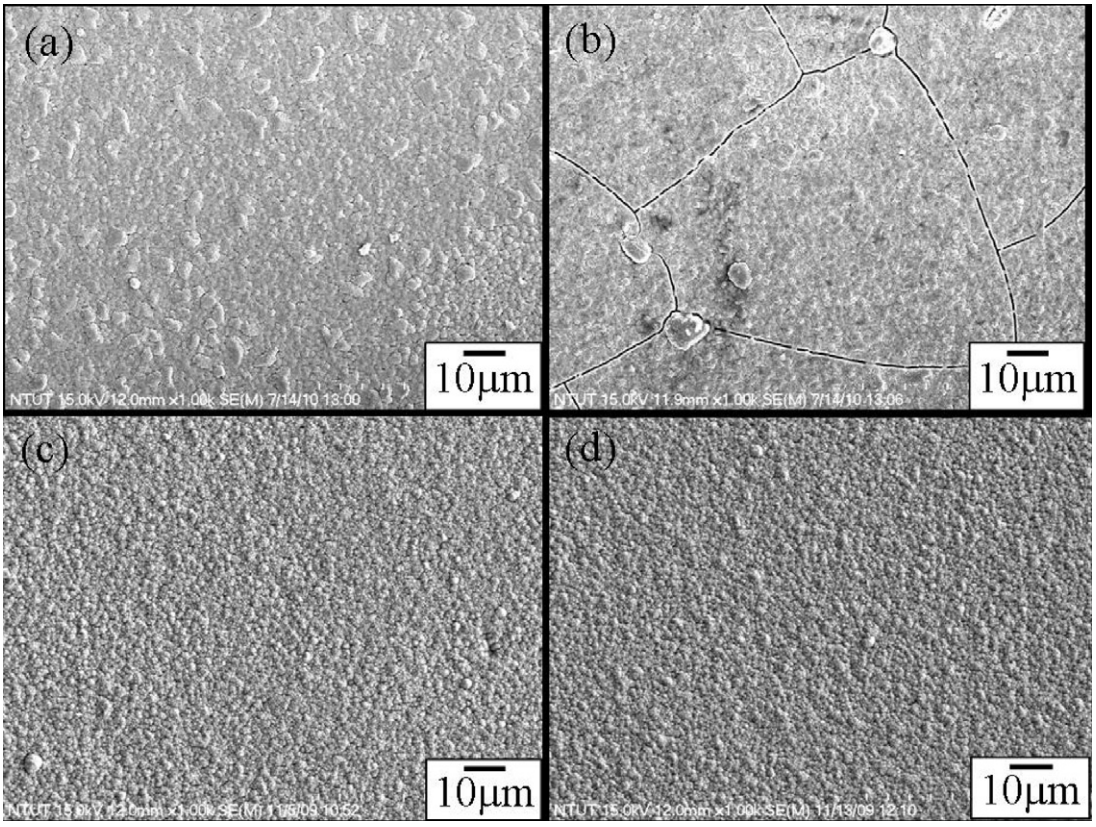

Figure 3. Surface SEM micrographs of BNO films deposited at (a) 25 °C and (c) 300 °C, and (b) and (d) the micrographs of corresponding films annealed at 700 °C for 2 h.

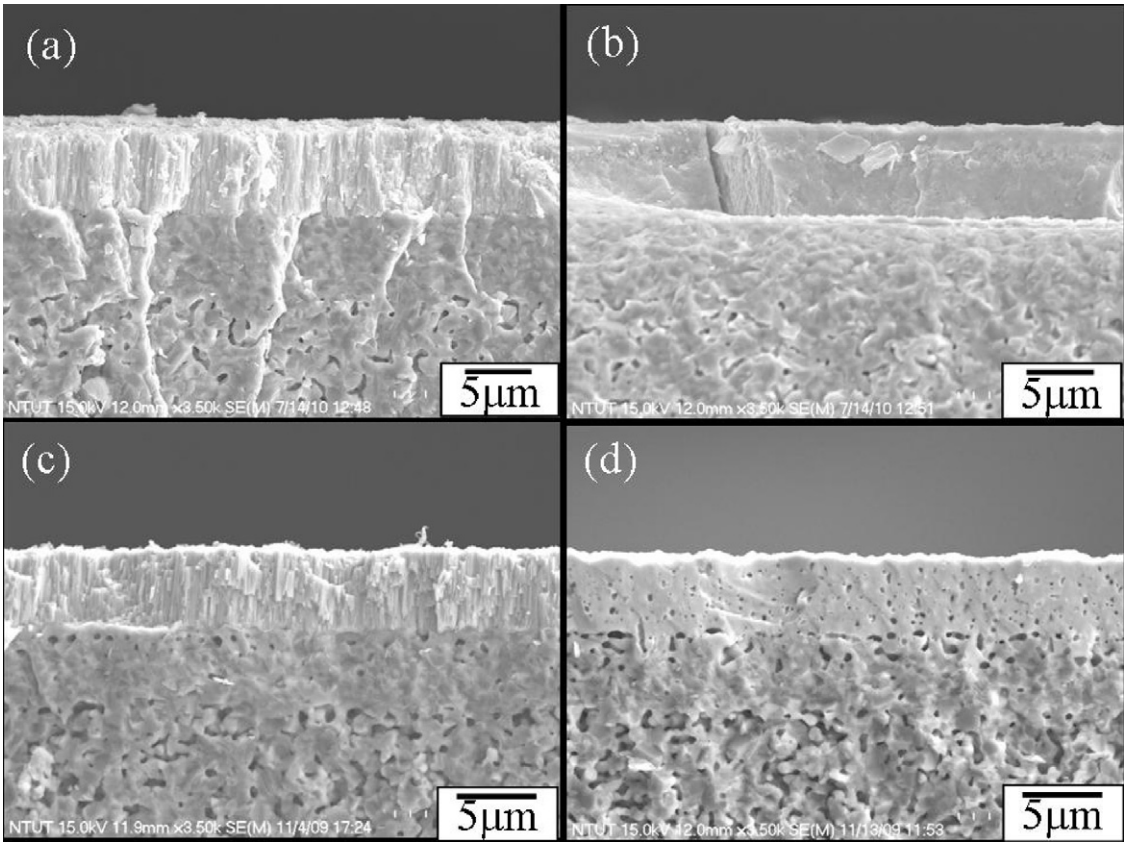

Figure 4. Cross-section SEM micrographs of BNO films deposited at (a) 25 °C and (c) 300 °C, and (b) and (d) the micrographs of corresponding films annealed at 700 °C for 2 h.

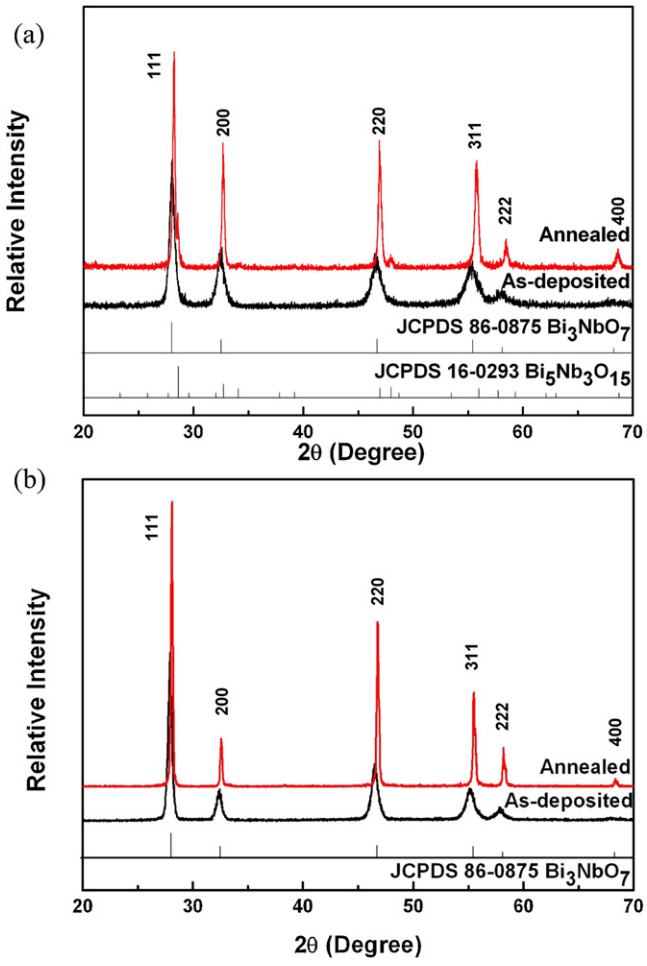

Figure 5. XRD patterns of BNO films deposited at (a) 25 °C and (b) 300 °C, and those followed by annealing at 700 °C for 2 h.

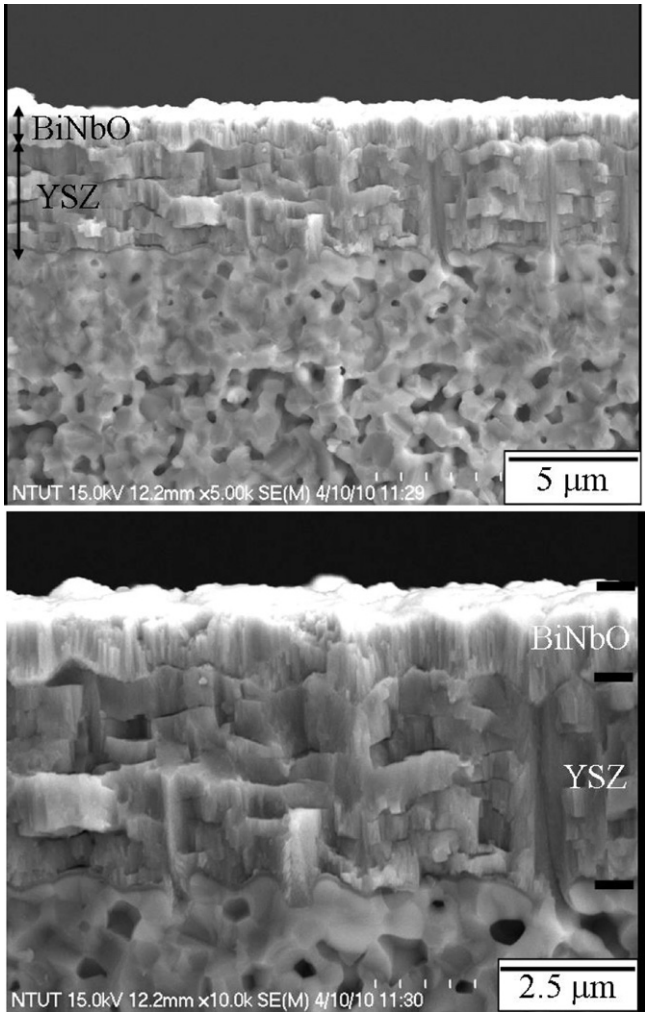

Figure 6. Cross-sections SEM micrographs of the anode-supported single cell containing a YSZ-BNO bi-layer electrolyte deposited by RF magnetron sputtering.

Figure 5 presents the XRD patterns of the as-deposited BNO films deposited at 25 °C and 300 °C, and the patterns of the films after annealing at 700 °C for 2 h. The as-deposited film was well-crystalline, with some broadening of x-ray peaks resulting from the fine grains and random orientation microstructure. No additional phases were detected in the films. After subsequent annealing at 700 °C, only Bi_3NbO_7 phase was observed for the film deposited at 300 °C. However, the major phase of Bi_3NbO_7 accompanied with trace amounts of $Bi_5Nbi_3O_{15}$ were observed in the film prepared at 25 °C [Figure 5(a)]. The intensities of the XRD peaks corresponding to Bi_3NbO_7 in both cases increase after annealing, implying a better crystallinity.

Figure 6 illustrates the cross-sections SEM micrographs of the anode substrate containing a YSZ-BNO bi-layer electrolyte deposited by RF magnetron sputtering. The interfaces among the anode, YSZ, and BNO layers showed no sign of crack, discontinuity, or delamination. The anode electrode consists of three layers with a total thickness of approximately 0.66 mm, including a current collector layer of NiO (≈20 μm) and two functional composite layers (with the NiO/SDC ratios of 60/40 wt% and 50/50wt%, and the thicknesses of ≈636 μm and ≈6 μm, respectively, as indicated in Table 1). The anode layers exhibited a porous microstructure while YSZ and BNO layers were fairly uniform in thickness (approximately 4.0 μm and 1.5 μm respectively). The cell performance of the anode supported SOFC with a YSZ-BNO bi-layer electrolyte deposited by RF magnetron sputtering and a screen-printed Ag cathode is shown in Figure 7. The cell reported a higher degree of concentration polarization as indicated by the convex-up curvature of the I-V curves at high current densities. The open circuit voltage (OCV) and the maximum power density of the single cell read respectively 0.94 V and 10 mW/cm^2 at 600 °C. The OCV value is lower than the expected theoretical value. Possible reasons for the deviation might include the gas leakage due to the pinholes formed in the bi-layer electrolytes and the partial electronic conductivity resulting in a short-circuited condition of the cell. The physical gas leakage can be excluded as a cause of decreased OCV, since the film is relatively dense based on the SEM observation. Although it is known in the literature that the electronic conductivity in bulk YSZ and BNO is negligibly small, it becomes significant with decreasing thickness due to an

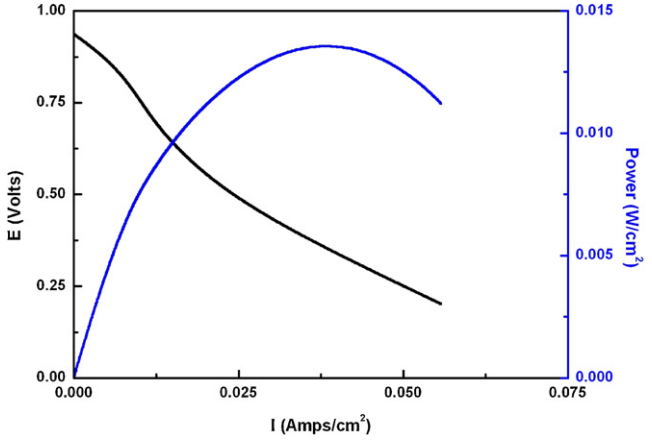

Figure 7. I-V curve and the corresponding power density of the anode supported single cell containing a YSZ-BNO bi-layer electrolyte at 6000 °C.

increased oxygen gradient [26,27]. At present, this seems to be the most reasonable explanation for the lower OCV.

4. Summary

YSZ-BNO bi-layer electrolyte films on NiO-SDC anode substrates were prepared by RF magnetron sputtering. The BNO film deposited in a mixture of 31 sccm Ar and 7 sccm O_2 appeared to be the closest to the target composition. The XRD patterns of the film are indexed to the cubic Fm $\bar{3}$ m structure of Bi_3NbO_7, which seems very similar to that of the target. The as-deposited film was well-crystalline and consisted of fine grains and random orientation microstructure. The single cell prepared consists of a bi-layer electrolyte of approximately 4.0 μm YSZ and 1.5 μm BNO layers, a NiO-SDC anode and an Ag cathode. The open circuit voltage (OCV) and the maximum power density (MPD) read 0.94 V and 10 mW/cm^2 at 600 °C respectively. The electronic conductivity associated with the thin electrolyte seems to be the most reasonable explanation for the lower OCV.

References

[1] M.D. Mata, X. Liub, Z. Zhu, B. Zhu, Development of Cathodes for Methanol and Ethanol Fuelled Low Temperature (300-600 °C) Solid Oxide Fuel Cells, International J. Hydrogen Energy 32 (2007) 796–801.
[2] J.H. Joo, G.M. Choi, Thick Film Electrolyte (Thickness< 20 μm)-Supported Solid oxide Fuel Cells, J. Power Sources 180 (2008) 195–198.
[3] E. Ivers-Tiffée, A. Weber, D. Herbstritt, Materials and Technologies for SOFC Components, Journal of the European Ceramic Society 21 (2001) 1805–1811.
[4] M. Zhang, M. Yang, Z. Hou, Y. Dong, M. Cheng, A Bi-Layered Composite Cathode of $La_{0.8}Sr_{0.2}MnO_3$-YSZ and $La_{0.8}Sr_{0.2}MnO_3$-$La_{0.4}Ce_{0.6}O_{1.8}$ for IT-SOFCs, Electrochimica Acta 53 (2008) 4998–5006.
[5] J.W. Fergus, Electrolytes for Solid Oxide Fuel Cells, J. Power Sources 162 (2006) 30–40.
[6] N. Jordan, W. Assenmacher, S. Uhlenbruck, V.A.C. Haanappel, H.P. Buchkremer, D. Stover, W. Mader, $Ce_{0.8}Gd_{0.2}O_{2-\delta}$ Protecting Layers Manufactured by Physical Vapor Deposition for IT-SOFC, Solid State Ionic 179 (2008).
[7] D. Yang, X. Zhang, S. Nikumb, C. Deces-Petit, R. Hui, R. Maric, D. Ghosh, Low Temperature Solid Oxide Fuel Cells with Pulsed Laser Deposited Bi-Layer Electrolyte, J. Power Sources 164 (2007) 182–188.
[8] Z. Zao, J. Huang, Z. Mao, C. Wang, Z. Liu, Preparation and Characterization of Nanocrystalline $Ce_{0.8}Sm_{0.2}O_{1.9}$ for Low Temperature Solid Oxide Fuel Cells Based on Composite Electrolyte, International J. Hydrogen Energy 35 (2010) 731–737.
[9] L. Liu, G.Y. Kim, A. Chandra, Fabrication of Solid Oxide Fuel Cell Anode Electrode by Spray Pyrolysis, J. Power Sources 195 (2010) 7046–7053.
[10] C.C. Chou, Y.B. Kim, F.B. Prinz, Surface Modification of Yttria-Stabilized Zirconia Electrolyte by Atomic Layer Deposition, Nano Letters 9 (2009) 3626–3628.
[11] A. Mineshige, K. Fukushima, K. Tsukada, M. Kobune, T. Yazawa, K. Kikuchi, M. Inaba, Z. Ogumi, Preparation of Dense Electrolyte Layer Using Dissociated Oxygen Electrochemical Vapor Deposition Technique, Solid State Ionics 175 (2004) 483–485.
[12] A. Tarancon, N. Sabate, A. Cavallaro, I. Gracia, J. Roqueta, I. Garbayo, J.P. Esquivel, G. Garcia, C. Cane, J. Santiso, Residual Stress of Free-Standing Membranes of Yttria-Stabilized Zirconia for Micro Solid Oxide Fuel Cell Applications, J. Nanoscience and Nanotechnology 10 (2010) 1327–1337.
[13] S. Charoirochkul, R.M. Rothian, K.L. Choy, B.C.H. Steele, Flame Assisted Vapor Deposition of Cathode for Solid Oxide Fuel Cells. 2. Modeling of Processing Parameters, J. Euro Ceram. Soc. 24 (2004) 2527–2535.
[14] J. Yan, X. Hou, K.L. Choy, The Electrochemical Properties of LSM-based Cathodes Fabricated by Electrostatic Spray Assisted Vapor Deposition, J. Power Sources 180 (2008) 373–379.
[15] X. Zhang, M. Robertson, C. Deces-Petit, Y. Xie, R. Hui, W. Qu, O. Kesler, R. Maric, D. Ghsoh, Solid Oxide Fuel Cells with Bi-layered Electrolyte Structure, J. Power Sources 175 (2008) 800–805.
[16] H. Moon, S.D. Kim, S.H. Hyun, H.S. Kim, Development of IT-SOFC Unit Cells with Anode-Supported Electrolytes via Tape casting and Co-firing, International J. Hydrogen Energy 33 (2008) 1758–1768.
[17] Y.J. Leng, S.H. Chan, K.A. Khor, S.P. Jiang, Performance Evaluation of Anode-Supported Solid Oxide Fuel Cells with Thin Film YSZ Electrolyte, International J. Hydrogen Energy 29 (2004) 1025–1033.
[18] K. Chen, Y. Tian, A. Lu, N. Ai, X. Huang, W. Su, Behavior of 3 mol% Yttria-Stabilized Tetragonal Zirconia Polycrystal Film Prepared by Slurry Spin Coating, J. Power Sources 186 (2009) 128–132.
[19] R.I. Tomova, M. Krauz, J. Jewulski, S.C. Hopkins, J.R. Kluczowski, D.M. Glowacka, B.A. Glowacki, Direct Ceramic Inkjet Printing of Yttria-Stabilized Zirconia Electrolyte Layers for Anode-Supported Solid Oxide Fuel Cells, J. Power Sources 195 (2010) 7160–7167.
[20] M. Matsuda, T. Hosomi, K. Murata, T. Fukui, M. Miyake, Fabrication of Bilayered YSZ/SDC Electrolyte Film by Electrophoretic Deposition for Reduced-Temperature Operating Anode-Supported SOFC, J. Power Sources 165 (2007) 102–107.
[21] Q. Ma, J. Ma, A. Zhou, R. Yan, J. Gao, G. Meng, A High-Performance Ammonia-Fuel SOFC Based on a YSZ Thin-Film Electrolyte, J. Power Sources 164 (2007) 86–89.
[22] L.R. Pederson, P. Singh, X.-D. Zhou, Application of Vacuum Deposition Methods to Solid Oxide Fuel Cells, Vacuum 80 (2006) 1066–1083.
[23] S.F. Wang, Y.R. Wang, C.T. Yeh, Y.F. Hsu, S.D. Chyou, W.T. Lee, Effects of Bi-layer LSCF-based Cathodes on Characteristics of Intermediate Temperature SOFCs, Journal of Power Sources 196 (2011) 977–987.
[24] R.S. Roth, T.L. Waring, J. Res. Nat. Bur. Stand., Sect 66A (1962) 451.
[25] I. Abrahams, A. Kozanecka-Szmigiel, F. Krok, W. Wrobel, S.C.M. Chan, J.R. Dygas, Correlation of Defect Structure and Ionic Conductivity in δ-phase Solid Solutions in the Bi_3NbO_7-Bi_3YO_6 System, Solid State Ionics 177 (2006) 1761–1765.
[26] J.S. Ahn, M.A. Camaratta, D. Pergolesi, K.T. Lee, H. Yoon, B.W. Lee, D.W. Jung, E. Traversa, E.D. Wachsman, Development of High Performance Ceria/Bismuth Oxide Bilayered Electrolyte SOFCs for Lower Temperature Operation, Journal of the Electrochemical Society 157 (2010) B376–B382.
[27] J. Yan, H. Matsumoto, T. Akbay, T. Yamada, T. Ishihara, Preparation of $LaGaO_3$-based Perovskite Oxide Film by a Pulsed-Laser Ablation Method and Application as a Solid Oxide Fuel Cell Electrolyte, J. Power Sources 157 (2006) 714–719.